Prominent ferroelastic domain walls in $BiVO_4$ crystal

1995 J. Phys.: Condens. Matter 7 7309

(http://iopscience.iop.org/0953-8984/7/37/005)

J. Phys.: Condens. Matter 7 (1995) 7309–7323. Printed in the UK

Prominent ferroelastic domain walls in $BiVO_4$ crystal

Ae Ran Lim†, Sung Ho Choh‡ and Min Su Jang§

† Department of Physics, Jeonju University, Chonju 560-759, Republic of Korea
‡ Department of Physics, Korea University, Seoul 136-701, Republic of Korea
§ Department of Physics, Pusan National University, Pusan 609-735, Republic of Korea

Received 16 February 1995, in final form 22 May 1995

Abstract. The domain structure of ferroelastic $BiVO_4$ crystals was investigated by x-ray diffraction, nuclear magnetic resonance, optical polarizing microscopy, transmission electron microscope, and electron diffraction techniques. From these results, it is found that the $BiVO_4$ crystals have only prominent W walls and no non-prominent W′ domain walls. A model of the twin structure is suggested, and all experimental results are explained in terms of this model. However, the prominent W wall obtained from our experimental results should not occur in the ferroelastic species $4/mF2/m$ previously reported. From the acoustic symmetry character of the elastic behaviour, it has been established that there exist two possible W and W′ walls for permissible planar walls that are consistent with all experimental observations. Thus, it can be concluded that the $BiVO_4$ crystals having only the W walls found by our group and W′ walls obtained by other groups are consistent with the ferroelastic species $4/mmmF2/m$ rather than $4/mF2/m$.

1. Introduction

Increasing applications for the ferroelastic bismuth vanadate ($BiVO_4$) crystal have been found in recent years. The crystal was first synthesized by Roth and Waring [1], and has received considerable attention since the discovery of a ferroelastic–paraelastic phase transition at 528 K by Bierlein and Sleight [2]. The transition is from a tetragonal scheelite structure (space group, $I4_1/a$) to a low-temperature monoclinic system (space group, $I2/a$) [3]. Recently, there have been a great many experimental investigations such as x-ray diffraction, neutron diffraction [4], and optical properties [5] to study the structural changes and the phase transition. Pinczuk *et al* [6] reported the Raman scattering at the transition temperature. David and Wood [7] extended the study on the ferroelastic phase transition of $BiVO_4$.

Ferroelastic domains occur necessarily in all ferroelastic crystals as a consequence of the reduction in symmetry between the paraelastic and ferroelastic phase. Sapriel [8] theoretically investigated the orientation of domain walls in ferroelastic crystals belonging to various crystal classes. According to him, the domain walls are classified into two kinds: the W wall and the W′ wall. The former has its orientation governed only by symmetry, no matter what values the strain components of the ferroelastic domain wall take. On the other hand, the latter has its orientation determined by the concrete values of the strain components. Since the discovery of ferroelasticity of $BiVO_4$, many experimental studies have been made in order to elucidate its domain structure. Previous authors [9–14] reported W′ domain walls in $BiVO_4$ following various experimental studies. Below 255 °C, two groups of W′ domain walls of $BiVO_4$ crystal are oriented at $91.5 \pm 0.5°$ to each other,

0953-8984/95/377309+15$19.50

which compares favourably with the calculated value of 91.14° obtained from the cell parameters [2]. The boundary was shown to be at the angle of $39 \pm 3°$ from the a axis from measurements under a polarizing microscope as reported by Sawada and Ishibashi [9]. The theoretically deduced angle 31.4° between the boundaries and the a axis is in good agreement with the observed value of 32° reported by Manolikas and Amelinckx [10]. From transmission electron microscope (TEM) and electron diffraction measurements, Wainer *et al* [11] reported the measured value of 37.4° corresponding to the $(1p0)$ plane with $p = 0.78$. Masanori *et al* [12] measured an angle of 39° with the [100] direction. These results agree reasonably well with the 36° orientation [13] calculated by Sapriel's formulae [8]. The relationship between the domain wall orientation and the spontaneous strain in ferroelastics was discussed, with particular reference to the W′ walls in $BiVO_4$, by David and Wood [14]. All reported results for the non-prominent W′ wall in a $BiVO_4$ crystal are summarized in table 1.

Table 1. The observed and calculated values of non-prominent W′ wall directions with respect to the [100] axis in a $BiVO_4$ crystal.

Reference	θ_{ob} (deg)	θ_{cal} (deg)	Experimental method
[9]	39		Polarizing microscope
[10]	32	31.4	TEM, electron diffraction
[11]	37.4	36	TEM, electron diffraction
[12]	39		
[13]		35	
[14]	37.4	36	

In our preceding paper [15], a prominent W wall in the $BiVO_4$ crystal was observed using x-ray diffraction and ^{51}V NMR: the domain boundary made an angle of 44.25° with respect to the a axis. The theoretical W and W′ wall orientations for permissible planar walls that are consistent with all experimental observations was discussed by Lim *et al* [16]. Two kinds of nearly perpendicular domain wall were observed using a polarizing microscope [17], and TEM [18]. The domain boundaries resulting from possible combinations of the four orientation states were also discussed by Lim *et al* [17]. From TEM and electron diffraction measurements [18], the angle obtained between [100] axis and the domain boundaries was $44 \pm 1°$. All reported results for the prominent W wall in a $BiVO_4$ crystal are summarized in table 2.

Table 2. The observed and calculated values of prominent W wall directions with respect to the [100] axis in a $BiVO_4$ crystal.

Reference	θ_{ob} (deg)	θ_{cal} (deg)	Experimental method
[15]	44.25		X-ray diffraction,^{51}V NMR
[16]		45	
[17]	44		^{51}V NMR, polarizing microscope
[18]	44		TEM, electron diffraction
[19]	44.2		Mn^{2+} EPR
Present work	44.25		^{209}Bi NMR

In this paper, we extend the theoretical analysis of the domain structures obtained by the x-ray diffraction, ^{51}V NMR, optical polarizing microscopy, TEM, and electron diffraction

methods. In addition, we have observed ^{209}Bi NMR in a $BiVO_4$ crystal having twin domains. Furthermore, we propose that $BiVO_4$ crystals having the W and W′ walls are consistent with all experimental observations of the ferroelastic species $4/mmmF2/m$ instead of $4/mF2/m$. This assignment is also supported by the Mn^{2+} ESR study in $BiVO_4$ [19].

2. Crystal structure

The $BiVO_4$ crystal is known to undergo a reversible second-order phase transition at T_c (= 528 K) between the ferroelastic fergusonite and the paraelastic scheelite structure [3]. In the paraelastic phase the structure is tetragonal as the lattice parameters determined at 573 K are $a = b = 5.1507$ Å, $c = 11.730$ Å, and $\gamma = 90.0°$ [20]. It was suggested that the point group is $4/m$ for $T > T_c$.

The ferroelastic phase of $BiVO_4$ has the point group $2/m$ with unit cell dimensions $a = 5.1966$ Å, $b = 5.0921$ Å, $c = 11.704$ Å, and $\gamma = 89.62°$ at room temperature [2]. There are two permissible orientations of the ferroelastic state, and, thus, twinning in the low-symmetry form is common.

3. Experimental procedure

$BiVO_4$ crystals were grown by melting a mixture of Bi_2O_3 (3N) and V_2O_5 (3N) powder. The crystals of the two types with either a single domain or twin domain were grown by the Czochralski method. Structures were confirmed by x-ray diffraction, and ^{51}V NMR [15]. A distinct cleavage plane perpendicular to the long [001] axis was observed in these crystals. This cleavage is not affected by twinning since the twin domain boundaries have a common direction along their [001] axis. A very striking change in colour of $BiVO_4$ crystals was observed at different temperatures. At liquid nitrogen temperature, the colour is pale yellow. As the temperature is raised this colour deepens, being orange at room temperature, deep red at 523 K, and purple at 773 K [21]. This process is completely reversible.

For the investigation of the relative orientation of the grains, a crystal goniometer for the back-reflection Laue camera was especially designed which was movable up to 10 cm right and left, and to 3 cm up and down, while the goniometer head was accurately maintained with respect to one reference direction.

A Varian model WL-112 wide-line spectrometer was used for the NMR measurement. The magnetic field was provided by an electromagnet with 30.5 cm pole diameter and 4.45 cm pole gap, up to the maximum field of 1.8 T. A Varian E-229 goniometer was employed for mounting the specimen. The high temperature was maintained by flowing nitrogen gas, heated using a home-made nichrome heater, over the sample.

The domain structure was examined by employing an optical polarizing microscope, a transmission electron microscope, and electron diffraction. The sample was a thin plate cut along the monoclinic (001) plane and polished with rouge. The sample was mounted on a transparent heating stage in order to observe the domain structure as a function of temperature.

4. Results and analysis

4.1. Twin structure determined by x-ray diffraction

Laue patterns were obtained at 10 different local points systematically chosen on the surface of the crystal. Selected patterns are shown in figure 1, where (*a*) shows the picture obtained

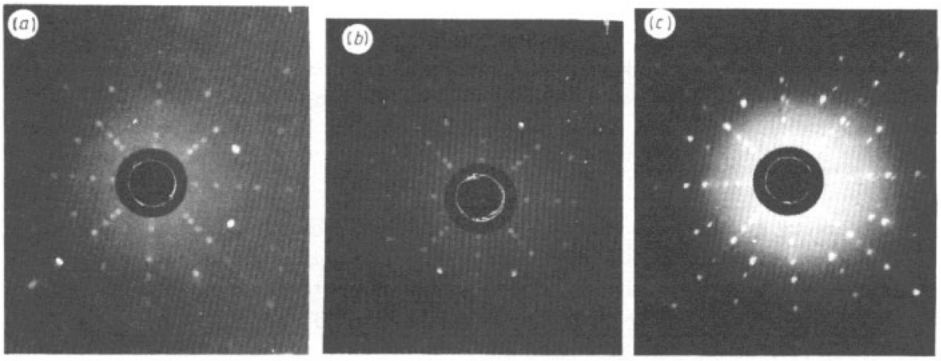

Figure 1. Back-reflection Laue patterns obtained with the incident beam antiparallel to the [001] axis. (*a*), (*b*), and (*c*) are described in the text.

at three points, (*b*) at five points, and (*c*) at the remaining two points.

The x-ray photograph shown in figure 1(*a*) was found to correspond to that with the x-ray beam directed in the [001] orientation from the (001) standard stereographic projection drawn with the crystallographic data $a = 5.1966$ Å, $b = 5.0921$ Å, $c = 11.704$ Å, and $\gamma = 89.62°$. The grains with the [001] orientation are denoted by A. The Laue picture in figure 1(*b*) was for the $[00\bar{1}]$ orientation coinciding with twofold rotation about the $[1\bar{1}0]_A$ axis [15]. The grains with the $[00\bar{1}]_B$ orientation are denoted by B. Analysis of 1(*c*) indicates a superposition of grains A and B with the [110] coaxis as shown in figure 2. The shape of the grains A and B was also examined by simultaneous x-ray Berg–Barrett reflection topography. Two simultaneous topographs of $(3\bar{2}7)_A$ and $(\bar{2}3\bar{6})_B$ planes were recorded with parallel stripes of black and white contrast. The information from these two topographs is displayed in figure 3.

The results for the three Laue patterns and two topographs in figures 1 and 3 show that the grains A and B are parallel to each other, and their domain structures are sketched in figure 4: their interfaces at boundaries are $(110)_A$ and $(\bar{1}\bar{1}0)_B$ planes.

The numbers 1 to 10 in figure 4 refer to the points at which the 10 Laue photographs were taken. Figure 1(*a*) was obtained from points marked 1, 3, and 5; 1(*b*) was from 4, 7, 8, 9, and 10; 1(*c*) was from 2 and 6.

4.2. Twin structure determined by ^{51}V NMR

^{51}V NMR data were obtained at a fixed frequency of 6 MHz in the ferroelastic phase. While the seven resonance lines (one group) of the ^{51}V ($I = \frac{7}{2}$) nucleus observed with the single-domain structure were reported previously [22], two groups of resonance lines are shown in figure 5. The signal intensity of one group is stronger than that of the other, but there are similarities between the two groups. The rotation patterns of the ^{51}V NMR spectra measured in the *ac* (and *bc*) plane are displayed in figure 6. Although the two patterns in figure 6 look different, they are simply related. From the data of the crystal with a single domain reported previously [22], it is found that the patterns in figure 6 are superposed on those in the *ac* plane (solid line) and *bc* plane (broken line) of the single domain. In particular, when the external magnetic field is applied along the *c* axis, the two groups of resonance lines coincide with those of the crystal with a single domain [22].

By using the quadrupole coupling constant, the asymmetry parameter, and the principal axes of the electric field gradient tensor of the crystal with a single domain ($X = a$, $Y = b$,

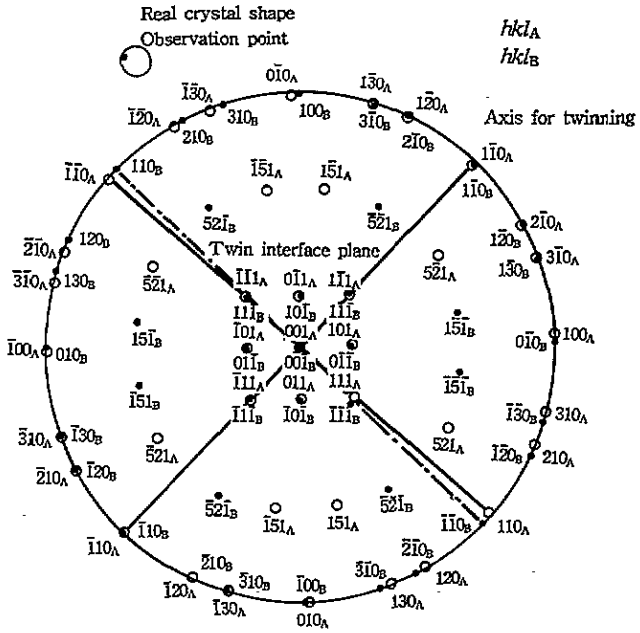

Figure 2. The superposed stereographic projection showing the relative orientations of grains A and B, oriented along $[001]_A$ and $[00\bar{1}]_B$, respectively.

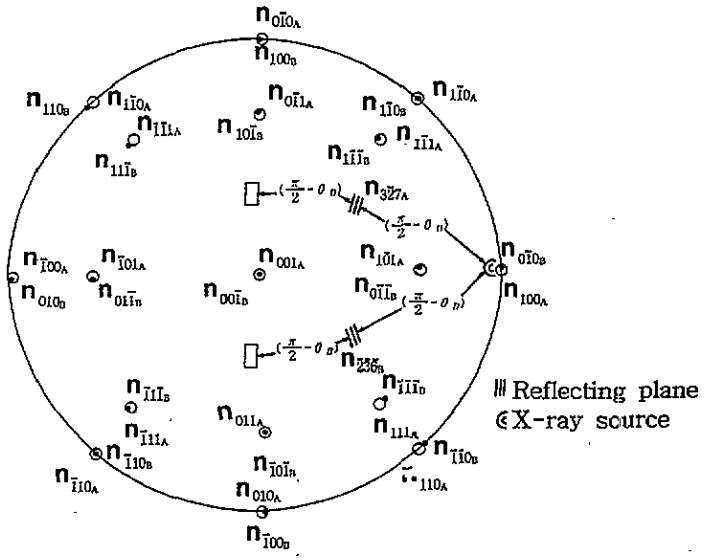

Figure 3. The superposed stereographic projection of $BiVO_4$ showing all the topographic information on the two simultaneous images of $(3\bar{2}7)_A$ and $(\bar{2}\bar{3}\bar{6})_B$ planes.

and $Z = c$) [22], the principal axis systems, the quadrupole coupling constant, and the asymmetry parameter of the two groups were analysed [15]. The quadrupole coupling constant and asymmetry parameter are found to be exactly the same except the direction of the principal axes. Furthermore, the principal axis systems are simply related, as shown

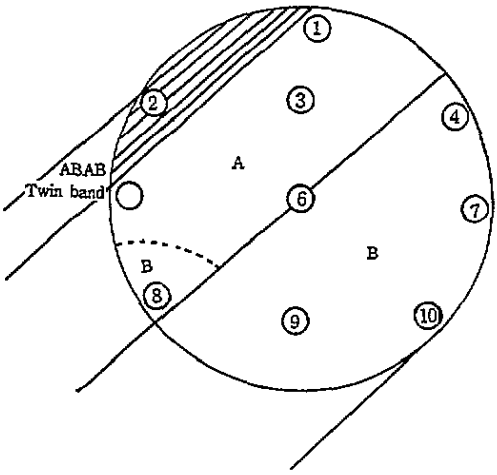

Figure 4. A schematic diagram of the twin structures in a $BiVO_4$ crystal. The numbers 1 to 10 indicate the local points where 10 back-reflection Laue photographs were taken.

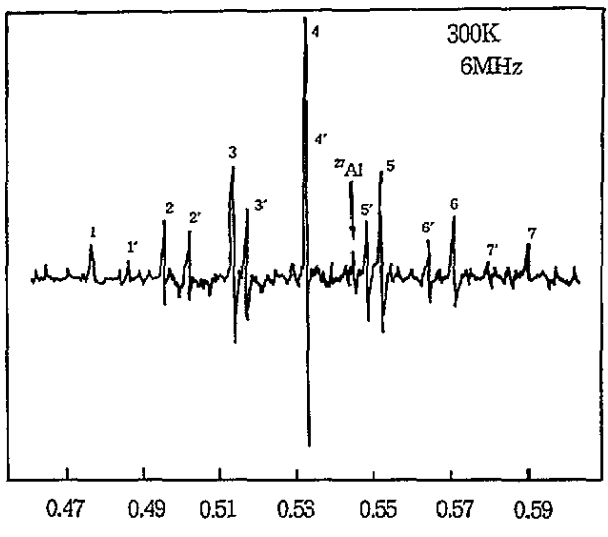

Figure 5. NMR spectra of ^{51}V in a $BiVO_4$ crystal. The magnetic field is applied along 50° from the *a* axis in the *ac* plane.

schematically in figure 7. The Z axis of one group (Z_1) is coincident with that of the other (Z_2), but the X_1 axis corresponds to the negative Y_2 axis and *vice versa*, where the subscript 1 (2) refers to the first (second) group.

In the paraelastic phase, the rotation patterns of ^{51}V NMR spectra measured in three mutually perpendicular planes [21] are displayed in figure 8. These patterns are similar to ^{51}V NMR with the single domain, and the resonance line of two groups displayed in the ferroelastic phase transformed into one group in the paraelastic phase. This result is consistent with the phase transition from the ferroelastic phase with the twin characteristic to the paraelastic phase which has no domains.

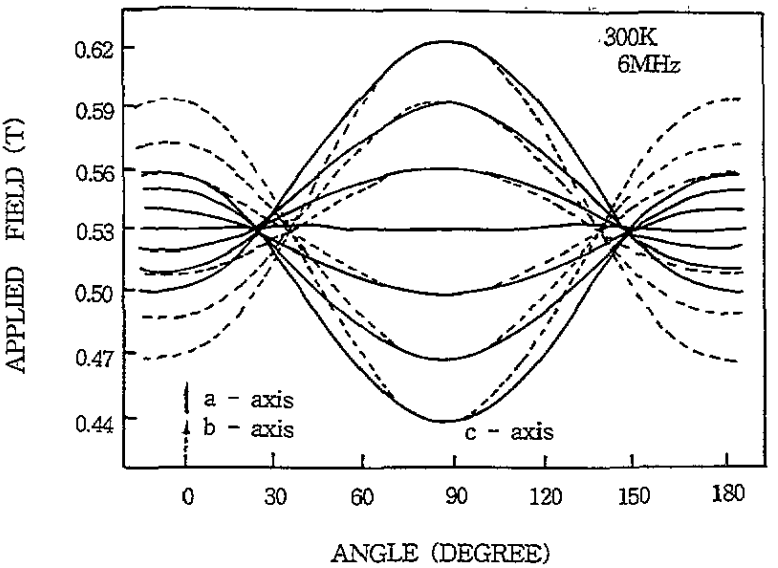

Figure 6. The rotation patterns of ^{51}V NMR in the *ac* plane for one group and the *bc* plane for the other group.

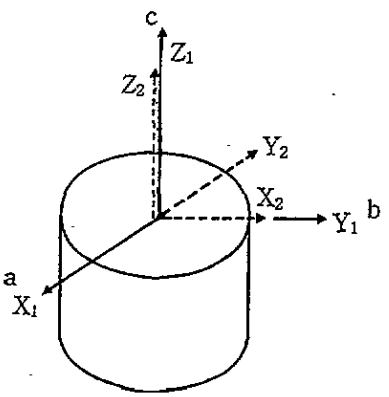

Figure 7. The relation between the two principal axes of the EFG tensor of the two groups for ^{51}V NMR.

4.3. Twin structure determined by ^{209}Bi NMR

^{209}Bi NMR data were also obtained at a fixed frequency of 6 MHz at room temperature. The nine-line structure was expected as a result of the quadrupole interaction of the ^{209}Bi ($I = \frac{9}{2}$) nucleus. A part of nine lines as one group of the ^{209}Bi nucleus were previously reported in the single domain [23]. However, two groups of resonance lines were measured in the twin-domain crystal. The rotation pattern of ^{209}Bi NMR spectra measured in the *ba* (and $\bar{a}b$) plane of the twin-domain crystal is shown in figure 9. The rotation pattern in figure 9 displays simultaneously one ^{209}Bi NMR and another displaced by 90°. The rotation patterns shown in figure 9 are superposed on those in the *ba* plane (solid line) and $\bar{a}b$ plane (broken line) of the single domain. The two groups of resonance lines measured in another crystallographic plane turned out to be not the principal plane of the EFG tensor. The maximum separation of the resonance line due to the quadrupole interaction was observed

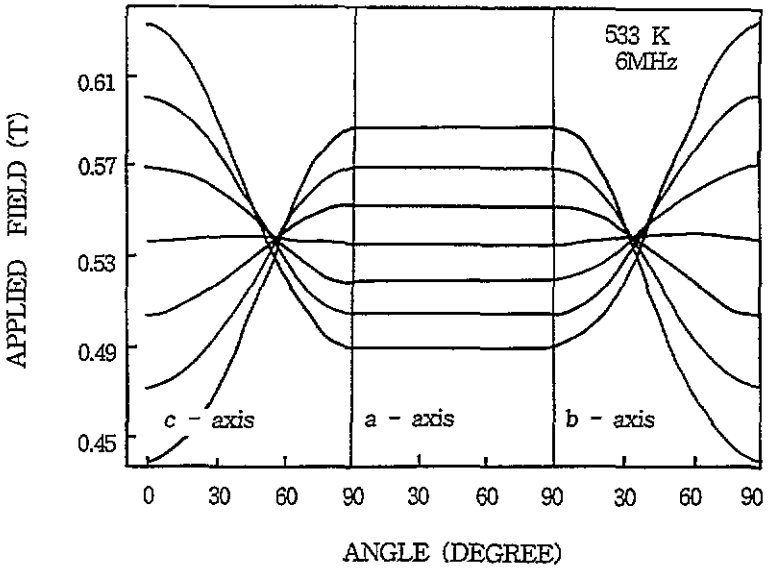

Figure 8. The rotation patterns of ^{51}V NMR measured in the three mutually perpendicular planes in the paraelastic phase.

when the magnetic field was applied along the c axis of the crystal and this direction is analysed to be the Z axis of the EFG tensor. The principal X, Y, and Z axes of the EFG tensor of ^{209}Bi in the ferroelastic phase are found to be along the crystallographic $a + 25°$, $b + 25°$, and c axis, respectively, for one group. The ^{209}Bi NMR lines in the twin-domain crystal are a superposition of the resonance lines of one domain and lines rotated by an angle 90° with respect to the c axis in the single-domain crystal. The relation between the principal axes of the EFG tensor of the two groups and the crystallographic axes is shown in figure 10.

The two sets of quadrupole parameters (the quadrupole coupling constant and asymmetry parameter) for the Bi ion in the twin-domain $BiVO_4$ are found to be the same except for the 90° discrepancy of the principal axes of the EFG tensor. The parameters obtained in the twin-domain crystal agree with those of the single-domain crystal [23]. From these results, one can deduce that the $BiVO_4$ single crystal possesses two distinctive domains, having the a axis in one domain parallel to the b axis in the other domain. NMR study of ^{51}V in $BiVO_4$ cannot differentiate between the b and $\bar{b}$ axis nor between the a and $\bar{a}$ axis because of the parallel relation between the principal axes of the EFG tensor and the crystallographic axes ($X||a$, $Y||b$, and $Z||c$). From ^{51}V and ^{209}Bi NMR study in the twin-domain crystal, a model of the twinning structure is suggested as shown in figure 11. Here, the X_V and Y_V axes are the principal axes of the EFG tensor for ^{51}V NMR, and the X_{Bi} and Y_{Bi} axes are those for ^{209}Bi NMR.

4.4. Twin structure examined by optical polarizing microscopy

Figure 12 shows an optical micrograph at room temperature of a $BiVO_4$ crystal containing domains [24]. This picture for the double-twin-domain crystal contains two nearly perpendicular parallel lines which are the domain walls. Furthermore, it is worth mentioning that this multidomain crystal is subdivided into two regions having two different groups of parallel lines [17]: a nearly horizontal group and a vertical one with much narrower spacing

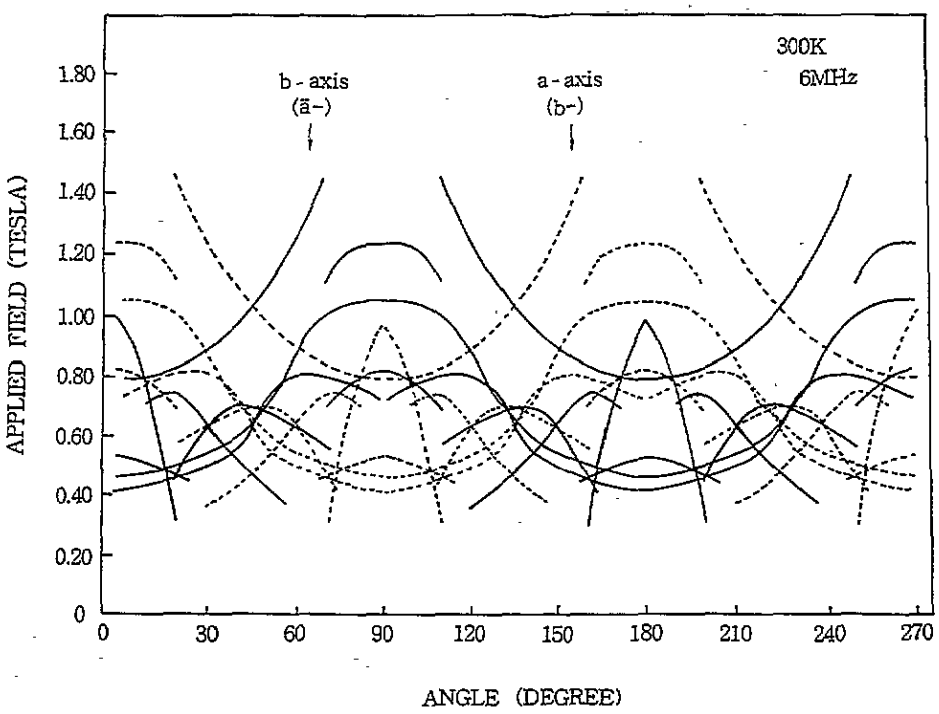

Figure 9. The rotation patterns of ^{209}Bi NMR in the *ba* plane for one group and the *āb* plane for the other group.

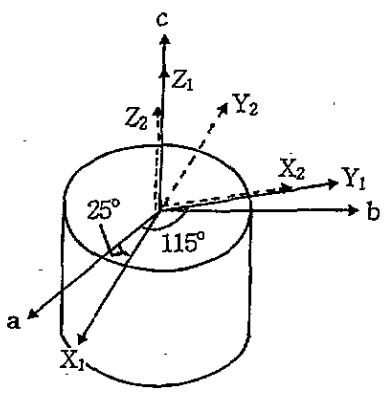

Figure 10. The relation between the two principal axes of the EFG tensor of the two groups for ^{209}Bi NMR.

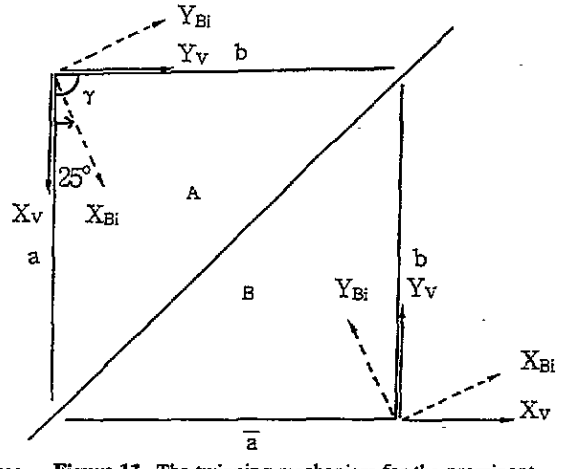

Figure 11. The twinning mechanism for the prominent W wall of $BiVO_4$ ($\gamma = 89.62°$).

between the lines. As the temperature was raised, the domain width broadened. The domain walls disappeared near T_c. On cooling, the domain walls reappeared again. This process is reversible.

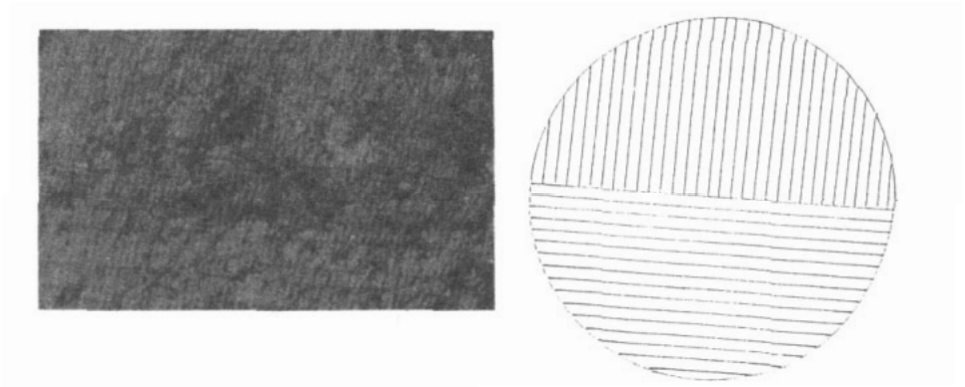

Figure 12. Domain wall in a $BiVO_4$ crystal having two nearly perpendicular parallel domains at room temperature (magnification ×200).

4.5. Twin structure determined by TEM and electron diffraction

A configuration of domain boundaries with two orientations separated by two nearly perpendicular groups of parallel lines is shown in figure 13. The pattern having two nearly perpendicular groups of parallel lines was similar to that observed by the optical polarizing microscopy mentioned above. A twofold splitting of the diffraction spots in the parallel domain wall was also observed by electron diffraction as shown in figure 14 [18]: the diffraction pattern taken from the circled area of figure 13. The spots shown in the diffraction pattern correspond to, as usual, the reciprocal lattice points.

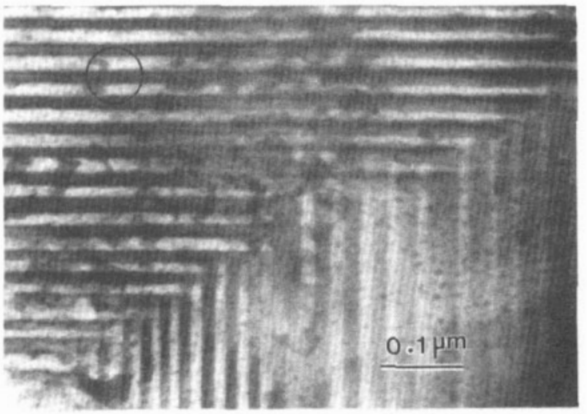

Figure 13. Bright-field micrograph with [001] zone axis, showing a typical configuration of domain boundaries separated by two nearly perpendicular groups of parallel lines.

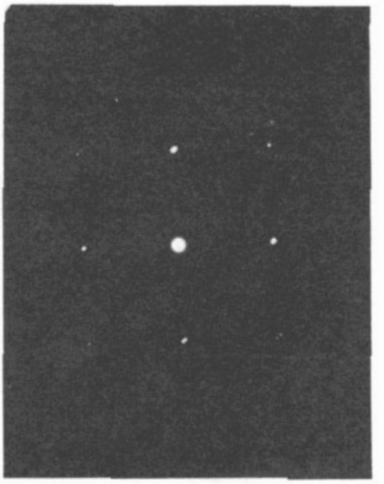

Figure 14. The pattern of electron diffraction taken from the domain boundary marked with a circle in figure 13.

A detailed schematic representation of the diffraction pattern is shown in figure 15. The direction of the splitting of two diffraction spots makes an angle $44 \pm 1°$ with respect to the a_2^* (or b_1^*) axis in reciprocal space: this is the angle between the a (or b) axis and

the domain boundaries in real space. Therefore, the measured value of the angle $44 \pm 1°$ between the [100] axis and the domain boundaries is that for the the prominent (110) W plane.

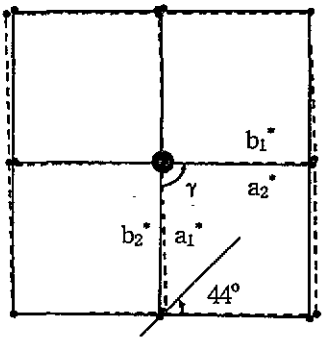

Figure 15. The twinning mechanism for the prominent W wall proposed by the diffraction pattern shown in figure 14, where the a^* (or b^*) is the axis in reciprocal space.

5. Discussion

The angle of the prominent W wall was obtained as 44° with respect to the [100] axis from the x-ray diffraction, NMR, TEM, and electron diffraction techniques. From these experimental results the model of the twin structure is presented as shown in figure 11. Therefore, we depict the detailed domain structure of the W plane as being formed with two nearly perpendicular groups of parallel lines (W_1 and W_2) as shown in figure 16. When the W_1 and W_2 walls are present, there are four orientation states related by a 90° rotation with respect to the c axis. When we analyse the structure of domain boundaries resulting from possible combinations of these four orientation states, we find that the boundary between the states 1 and 1* is the W_1 wall and the W_2 wall is between 2 and 2*. Using the strain compatibility criterion given by Sapriel [8], we find that states 1 and 2 can be matched along any direction (the same for 1* and 2*), i.e., no preferential boundary exists between them. On the other hand, states 1 and 2* (or 1* and 2) cannot be matched by a 90° rotation with respect to the c axis. The orientation states 1 and 1*, and 2 and 2* are separated by the W_1 wall and W_2 wall, respectively. Nevertheless, the orientation states 1 and 2*, and 1* and 2, respectively, are magnetically equivalent, beacause the a axis direction of orientation state 1 is different from that of orientation state 2* by an angle of 180° and the $BiVO_4$ crystal has a twofold symmetry about the c axis. Therefore, only two groups of NMR lines are expected as confirmed by the ^{51}V and ^{209}Bi NMR results. When the two nearly perpendicular groups of parallel domain walls are obtained by the optical polarizing microscope and TEM, two groups of resonance lines of ^{51}V and ^{209}Bi NMR are also recorded. These results are found to be related to the facts that the crystallographic a and b axis of one domain 1 (1*) are rotated by an angle 90° to be the crystallographic a and b axis of the other domain 2 (2*), and the c axis of the $BiVO_4$ crystal has a twofold symmetry.

However, the domain walls in $BiVO_4$ reported by previous authors [9–14] were the W′ wall with the angle of 36° between the [100] crystallographic direction at room temperature. In order to understand the structure of the prominent W wall obtained from our experimental results [15–19] and the non-prominent W′ wall reported by previous other groups [9–14], we have discussed two possible types of permissible domain wall using the elastic constants to explain why the domain walls have certain structural orientations.

In principle, the domain wall directions in $BiVO_4$ can be determined from elastic

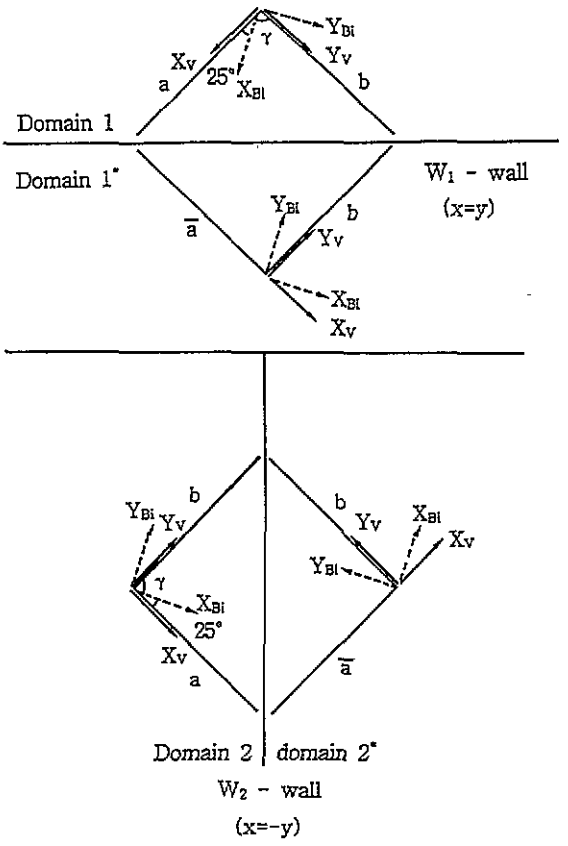

Figure 16. Ferroelastic domain structure formed by two nearly perpendicular groups of parallel domain walls. Here, the X_V and Y_V axes are the principal axes of the EFG tensor for ^{51}V NMR, and the X_{Bi} and Y_{Bi} axes are the principal axes of the EFG tensor for ^{209}Bi NMR.

constants [25]. The elastic constants of the $4/m$ crystal may be obtained from the values of the velocities of ultrasonic waves [26]. Scheelite structure crystals have $4/m$ Laue symmetry and normally their elastic constants are referred to an XYZ axis set in which the Z axis is parallel to the fourfold axis [27]. It is common practice for the centrosymmetrical elastic stiffness constant tensors (C_{ijkl}) to divide tetragonal crystals into two Laue groups: $4/mmm$ (TI) and $4/m$ (TII). In a conventional crystallographic axis system, the higher-symmetry crystals belonging to the TI group (the constituent point groups are $4mm$, 422, $4\bar{2}m$, and $4/mmm$) have six independent elastic stiffness constants. We use the generally accepted replacement of pairs for indices of components of the tensor C_{ijkl} by one index such that $11 \rightarrow 1$, $22 \rightarrow 2$, $33 \rightarrow 3$, $23\ (32) \rightarrow 4$, $13\ (31) \rightarrow 5$, and $12\ (21) \rightarrow 6$ [28], then

$$(C_{ij}) = \begin{bmatrix} C_{11} & C_{12} & C_{13} & 0 & 0 & 0 \\ C_{12} & C_{11} & C_{13} & 0 & 0 & 0 \\ C_{13} & C_{13} & C_{33} & 0 & 0 & 0 \\ 0 & 0 & 0 & C_{44} & 0 & 0 \\ 0 & 0 & 0 & 0 & C_{44} & 0 \\ 0 & 0 & 0 & 0 & 0 & C_{66} \end{bmatrix}. \tag{1}$$

The reference set $(+X, +Y, +Z)$, orthogonal, right-handed, and axial includes the Z axis

parallel to the fourfold axis, and the X and Y axes are then in the Z plane along the a and b crystallographic axes, respectively. The presence of vertical planes of symmetry or diad axes in the Z plane imposes the condition that C_{16} should be zero.

This is not the case for crystals of the TII group (the constituent point groups are 4, $\bar{4}$, and $4/m$) for which the elastic stiffness constant matrix referred to the frame of the crystallographic axes (a, b, c) is

$$(C_{ij}) = \begin{bmatrix} C_{11} & C_{12} & C_{13} & 0 & 0 & C_{16} \\ C_{12} & C_{11} & C_{13} & 0 & 0 & -C_{16} \\ C_{13} & C_{13} & C_{33} & 0 & 0 & 0 \\ 0 & 0 & 0 & C_{44} & 0 & 0 \\ 0 & 0 & 0 & 0 & C_{44} & 0 \\ C_{16} & -C_{16} & 0 & 0 & 0 & C_{66} \end{bmatrix}. \tag{2}$$

The non-zero value of C_{16} in the $4/m$ (TII) Laue crystals gives rise to apparently more complicated elastic behaviour than that is found for the $4/mmm$ (TI) Laue symmetry. For this special case of tetragonal crystals, Khatkevich [29], and Blanchfield and Saunders [30], showed that the usual requirement of seven elastic tensor components to describe the elastic behaviour of tetragonal $4/m$ (TII) crystals could be reduced to six parameters when referred to a suitable choice of reference frame. This was also shown in $BiVO_4$ [16].

In the tetragonal scheelite structure of $BiVO_4$, the isolated VO_4 tetrahedra have a point symmetry $\bar{4}$. The fourfold axis of tetrahedra makes an angle $\phi_k = 28.97°$ with respect to the [100] direction. This angle, called the setting angle [31], has been shown to be related to the components of elastic constants along the k and γ axes of the acoustic symmetry, respectively [27]. The transformation of the components of the elastic tensor of the $4/m$ (TII) crystal due to a rotation about the Z axis through an angle ϕ_k makes C_{16} equal to zero, and consequently yields a tensor form of $4/mmm$ (TI) materials. From these results, the elastic properties referred to the acoustic symmetry axes of tetragonal $BiVO_4$ are identical to those of $4/mmm$ (TI) and $4/m$ (TII) point group symmetry [27, 29, 32].

David and Wood [14] reported that the $BiVO_4$ crystal belongs to the ferroelastic species $4/mF2/m$; the paraelastic and the ferroelastic phases have $4/m$ and $2/m$ symmetry, respectively, and F represents the ferroelastic phase. For the ferroelastic species $4/mF2/m$, the spontaneous monoclinic distortion takes the following form:

$$\begin{bmatrix} -f & g & 0 \\ g & f & 0 \\ 0 & 0 & 0 \end{bmatrix} = \begin{bmatrix} (\varepsilon_{11} - \varepsilon_{22})/2 & \varepsilon_{12} & 0 \\ \varepsilon_{12} & -(\varepsilon_{11} - \varepsilon_{22})/2 & 0 \\ 0 & 0 & 0 \end{bmatrix} \tag{3}$$

where ε_{11}, ε_{22}, and ε_{12} are determined from the monoclinic (m) and tetragonal (t) lattice parameters measured at temperature T;

$$\begin{aligned} \varepsilon_{11}(T) &= (a_m(T) - a_t(T))/a_m(T) \\ \varepsilon_{22}(T) &= (b_m(T) - b_t(T))/b_m(T) \\ \varepsilon_{12}(T) &= \tan[(\gamma_m - 90°)/2]. \end{aligned} \tag{4}$$

Consequently, the orientation of domain walls can be derived as follows[8]:

$$f(x^2 - y^2) - 2gxy = 0. \tag{5}$$

The solution of equation (5) gives

$$x = py \qquad x = -y/p$$

where

$$p = [g + (f^2 + g^2)^{1/2}]/f. \tag{6}$$

Using the spontaneous strain tensors given by Aizu [33] and the formulae proposed by Sapriel [8], we can evaluate the domain wall orientations.

In the case of the transition from $4/mmm$ to $2/m$ symmetry, the domain wall orientations are expressed by the following equations [8]:

$$\begin{array}{ll} \mathrm{W}' & x = py \quad \text{and } x = -y/p \\ & x = -py \quad \text{and } x = y/p \end{array} \tag{7}$$

and

$$\begin{array}{ll} \mathrm{W} & x = 0 \quad \text{and } y = 0 \\ & x = y \quad \text{and } x = -y. \end{array} \tag{8}$$

These directions lie along the crystallographically prominent W wall as well as the non-prominent W′ wall. Using the monoclinic axis system, we have shown that the non-prominent domain walls are the $(1p0)$ planes with p given by equation (6). The calculated angles of the domain wall were obtained by a suitable choice of lattice parameters as indicated. In addition to the non-prominent W′ wall, the prominent W wall with $x = y$ and $x = -y$ is also permissible [16]. Therefore, the W wall makes an angle of 45° with respect to the [100] axis.

The formation of single- or twin-domain crystals seems to be dependent on the conditions of crystal growth. Natural $BiVO_4$ single crystals, occurring as the mineral pucherite, are known to have an orthorhombic structure. Apparently, laboratory syntheses have never achieved this modification. Low-temperature syntheses produce a tetragonal zircon-type $BiVO_4$ and high-temperature syntheses result in a monoclinic form of $BiVO_4$. Consequently, $BiVO_4$ single crystals may have different crystal structures according to the conditions of the natural and laboratory syntheses.

6. Conclusion

The domain structure of the ferroelastic $BiVO_4$ crystals has been studied by x-ray diffraction, ^{51}V and ^{209}Bi NMR, optical polarizing microscope, TEM, and electron diffraction techniques. From these experimental results, we have established that the $BiVO_4$ crystal has a prominent W wall. A model of the twin structure for this crystal is suggested.

The twin-domain crystal grown by our group has only prominent W domain walls (one or two W planes) and no non-prominent W′ domain walls. However, the prominent W wall obtained from our experimental results should not occur in the ferroelastic species $4/mF2/m$ previously reported. We have established that there exist two possible W and W′ walls for permissible planar walls from the ferroelastic species $4/mmmF2/m$. Thus, we may conclude that the $BiVO_4$ crystals having only W walls found by our group and W′ walls obtained by other groups are consistent with the ferroelastic species $4/mmmF2/m$ rather than $4/mF2/m$.

Acknowledgments

This work is supported by the Basic Science Research Institute Program, Ministry of Education, 1994, project No BSRI-94-2410 and in part by the Korea Science and Engineering Foundation (KOSEF) through the Research Center for Dielectric and Advanced Matter Physics (RCDAMP) at Pusan National University (1994–1997).

References

[1] Roth R S and Waring J L 1963 *Am. Mineral.* **48** 1348
[2] Bierlein J D and Sleight A W 1975 *Solid State Commun.* **16** 69
[3] Sleight A W, Chen H Y and Ferretti A 1979 *Mater. Res. Bull.* **14** 1571
[4] David W I F, Glazer A M and Hewat A W 1979 *Phase Transitions* **1** 155
[5] Aubry S and Pick R 1971 *J. Physique* **32** 657
[6] Pinczuk A, Welber B and Dacol F H 1979 *Solid State Commun.* **29** 515
[7] David W I F and Wood I G 1983 *J. Phys. C: Solid State Phys.* **16** 5093
[8] Sapriel J 1975 *Phys. Rev.* B **12** 5128
[9] Sawada A and Ishibashi Y 1979 *Kotai Butsuri* **14** 464
[10] Manolikas C and Amelinckx S 1980 *Phys. Status Solidi* a **60** 167
[11] Wainer L S, Baggio R F, Dussel H L and Benyacar M A R 1981 *Ferroelectrics* **31** 121
[12] Masanori C, Toshirou Y, Takashi F, Akikatsu S and Yoshihiro I 1982 *J. Phys. Soc. Japan* **51** 2914
[13] Mnushkina I E and Dudnik E F 1982 *Sov.–Phys. Crystallogr.* **27** 485
[14] David W I F and Wood I G 1983 *J. Phys. C: Solid State Phys.* **16** 5149
[15] Moon E Y, Choh S H, Park Y H, Yeom H Y and Jang M S 1987 *J. Phys. C: Solid State Phys.* **20** 1867
[16] Lim A R, Choh S H and Jang M S 1989 *J. Phys.: Condens. Matter* **1** 1571
[17] Lim A R, Choh S H and Jang M S 1990 *J. Korean Phys. Soc.* **23** 162
[18] Lim A R, Lee K H and Choh S H 1992 *Solid State Commun.* **83** 185
[19] Yeom T H, Choh S H, Song K J and Jang M S 1994 *J. Phys.: Condens. Matter* **6** 383
[20] Dudnik E P, Gene B B and Menushkina I E 1979 *Izv. Akad. Nauk.* **43** 1723
[21] Lim A R, Choh S H and Jang M S 1989 *Ferroelectrics* **94** 389
[22] Choh S H, Moon E Y, Park Y H and Jang M S 1985 *Japan. J. Appl. Phys.* **24** 640
[23] Lim A R, Choh S H and Jang M S 1992 *J. Phys.: Condens. Matter* **4** 1607
[24] Lim A R, Choh S H and Jang M S 1988 *Sae Mulli (New Phys.)* **28** 611
[25] David W I F 1983 *J. Phys. C: Solid State Phys.* **16** 2455
[26] Chung D Y and Li Y 1971 *Phys. Status Solidi* a **5** 669
[27] Farley J M, Saunders G A and Chung D Y 1975 *J. Phys. C: Solid State Phys.* **8** 780
[28] Nye J F 1967 *Physical Properties of Crystals* (Oxford: Oxford University Press) ch IV
[29] Khatkevich A G 1962 *Sov.–Phys. Crystallogr.* **6** 561
[30] Blanchfield P and Saunders G A 1979 *J. Phys. C: Solid State Phys.* **12** 4673
[31] David W I F 1983 *J. Phys. C: Solid State Phys.* **16** 5119
[32] Farley J M, Saunders G A and Chung D Y 1973 *J. Phys. C: Solid State Phys.* **6** 2010
[33] Aizu K 1970 *J. Phys. Soc. Japan* **28** 706